applied sciences

MDPI

Article

Synthesis, Physical Properties and Electrochemical Applications of Two Ionic Liquids Containing the Asymmetric (Fluoromethylsulfonyl)(Trifluoromethylsulfonyl)imide Anion

Oriele Palumbo [1,*], Giovanni Battista Appetecchi [2], Giovanna Maresca [2], Jean-Blaise Brubach [3], Pascale Roy [3], Simone Di Muzio [1], Francesco Trequattrini [1,4], Delphine Bordignon [5], Florine Legrand [5], Anaïs Falgayrat [5], Rongying Lin [5], Sebastien Fantini [5] and Annalisa Paolone [1]

[1] Consiglio Nazionale delleRicerche, Istituto dei Sistemi Complessi, Piazzale Aldo Moro 5, 00185 Rome, Italy; simone.dimuzio@libero.it (S.D.M.); francesco.trequattrini@roma1.infn.it (F.T.); annalisa.paolone@roma1.infn.it (A.P.)
[2] Agenzia Nazionale per le Nuove Tecnologie, l'Energia e lo Sviluppo Economico Sostenibile (ENEA), Materials and Physicochemical Processes Technical Unit (SSPT-PROMAS-MATPRO), Via Anguillarese 301, 00123 Rome, Italy; gianni.appetecchi@enea.it (G.B.A.); giovanna.maresca@uniroma1.it (G.M.)
[3] Synchrotron SOLEIL, L'Orme des Merisiers Saint-Aubin, CEDEX BP 48, 91192 Gif-sur-Yvette, France; jean-blaise.brubach@synchrotron-soleil.fr (J.-B.B.); pascale.roy@synchrotron-soleil.fr (P.R.)
[4] Dipartimento di Fisica, Sapienza Università di Roma, Piazzale Aldo Moro 5, 00185 Rome, Italy
[5] Solvionic SA, 11 Chemin des Silos, 31100 Toulouse, France; dbordignon@solvionic.com (D.B.); flegrand@solvionic.com (F.L.); afalgayrat@solvionic.com (A.F.); rlin@solvionic.com (R.L.); sfantini@solvionic.com (S.F.)
* Correspondence: oriele.palumbo@roma1.infn.it

Abstract: Novel ionic liquid (IL) electrolytes based on the asymmetric (fluoromethylsulfonyl) (trifluoromethylsulfonyl)imide $(FTFSI)^-$ anion, combined with the *N*-trimethyl-*N*-butyl-ammonium $(N1114)^+$ and *N*,*N*-diethyl-*N*-methyl-*N*(2-methoxyethyl)-ammonium $(N122(2O1))^+$ cations, were successfully synthesized and investigated in terms of thermal, vibrational and electrochemical properties. Thermogravimetric measurements revealed that the ionic liquids are stable up to 300 °C (2% mass loss). Differential scanning calorimetry measurements evidenced no phase transition down to −90 °C, suggesting a transition towards a glass state at lower temperatures. Infrared spectroscopy measurements, for the first time performed on ILs containing FTFSI, could not detect any crystallization down to −140 °C. The frequency of the main absorption bands of the ILs are in good agreement with DFT calculations. The FTFSI ionic liquid electrolytes, containing 20% mol of LiTFSI, show no solid-liquid phase transition due to the asymmetry of the $FTFSI^-$ anion, increasing the −10 °C conductivity up to 10^{-4} S cm^{-1}. These interesting ion transport properties remarkably extend the operative temperature range down to low temperatures. The FTFSI electrolytes exhibit remarkable electrochemical stability up to 4.8 V, this making them appealing for realizing safer and highly reliable lithium battery systems operating at high voltages.

Keywords: FTFSI; ionic liquids; asymmetric anions; thermal properties; ionic conductivity

check for updates

Citation: Palumbo, O.; Appetecchi, G.B.; Maresca, G.; Brubach, J.-B.; Roy, P.; Di Muzio, S.; Trequattrini, F.; Bordignon, D.; Legrand, F.; Falgayrat, A.; et al. Synthesis, Physical Properties and Electrochemical Applications of Two Ionic Liquids Containing the Asymmetric (Fluoromethylsulfonyl) (Trifluoromethylsulfonyl)imide Anion. *Appl. Sci.* **2022**, *12*, 4524. https://doi.org/10.3390/app12094524

Academic Editor: Dong-Won Kim

Received: 28 March 2022
Accepted: 28 April 2022
Published: 29 April 2022

1. Introduction

Ionic liquids (ILs) have a long history [1], but they were the object of a rapid increase in interest in the last 25 years [1], witnessed also from the development of industrial processes involving ILs [2]. In general, they possess peculiar properties, such as a low vapor pressure, high thermal and electrochemical stability, large liquid ranges that can extend below room temperature, high ionic conductivity and good solubility properties; therefore, they were proposed for uncountable applications [3–6], such as solvents, electrolyte components, lubricants and heat transfer media.

Electrochemistry is one of the most studied application for ILs, as they are considered as valid alternatives to the more usual organic alkyl-carbonates, which are the main components of lithium cell electrolytes [6]. In the last years, the application of batteries to the automotive sector has pushed research towards innovative cells, with even higher energy and power densities, that need novel materials to fulfill these requirements. In this framework, ILs have the potentiality to highly surpass the performances of organic solvents because of their higher thermal stability, non-flammability and larger anodic stability [6]. High energy and power density values in general require the use of materials at higher operative voltages (around 5 V).

There is a limited number of ILs that can work at such high potentials without the occurrence of decomposition (oxidation), and all of them contain highly fluorinated anions. The most widely used anions are bis(trifluoromethylsulfonyl)imide (TFSI) and bis(fluorosulfonyl)imide (FSI). However, other fluorinated anions, such as (trifluoromethanesulfonyl) (nonafluorobutanesulfonyl)imide (IM14), (difluoroethanesulfonyl)(nonafluorobutanesulfonyl) imide (IM24), (nonafluorobutanesulfonyl)(toluenesulfonyl)imide, (IMT4) and 1,3-hexafluoropropane-disulfonylimide (IM3) were also investigated, providing good electrochemical performances [7]. Moreover, the fluorosulfonyl-(trifluoromethanesulfonyl)imide (FTFSI) asymmetric anion was additionally proposed [8].

The first study on FTFSI-based ILs reported a thermal stability above 250 °C, a strong resistance to crystallization, values of ionic conductivity above 10^{-4} S cm^{-1} even at −40 °C and an electrochemical stability exceeding 5 V [8]. The use of FTFSI-containing ILs was also studied in dual-ion cells, in comparison with liquids based on the TFSI anion [9,10]. Some studies were devoted to the investigation of the anodic stability of the aluminum current collectors for high voltage supercapacitors [11], sodium [12] or lithium cells [13] in the presence of FTFSI-based ILs. This class of Ils was also used as components of polymeric electrolytes based on polyethylene oxide [14,15]. Concentrated electrolytes composed of LiFTFSI, LiFSI and ether solvents were reported for improving the cycling stability of lithium metal and inhibiting Li-metal dendritic growth [16]. ILs combining alkoxy-functionalized ammonium cations with asymmetric FTFSI anions seem to give rise to optimized ILs with improved fluidity [17]. FTFSI ILs were used as electrolytes also in combination with organic carbonates, providing some eutectic composition [18,19]. Certain recent studies were devoted to the investigation of the Solid-Electrolyte Interphase (SEI) developed when FTFSI-based ILs are used as electrolytes [20,21] or components of a polymer electrolyte [15]. The TFSI and FTFSI salts are reported to lead to thicker, more highly passivating surfaces than those developed in the presence of FSI salts [20]. Ionic liquids based on the FTFSI anion, combined with the trimethyl-isobutyl-ammonium cation $(N111i4)^+$, have shown interesting physicochemical and electrochemical properties and the ability of keeping in a super-cooled state for more than one year [22]. However, LiFTFSI and LiFSI salts are favorable for forming less dendritic, denser and more compact lithium metal deposits [15]. In particular, the SEI layer in LiFTFSI-based electrolytes contains an optimum amount of inorganic species (mainly LiF), a prerequisite for a mechanically and electrochemically stable SEI layer [15]. In cells containing a Si anode and a Ni-rich layered oxide cation, the decomposition of the (fluorosulfonyl)(trifluoromethanesulfonyl)imide (FTFSI) anions leads to a LiF- and Li_3N-rich SEI [21]. The development of passivation films on LiF was also computationally investigated by Rigoni et al., because lithium fluoride is one of the main components of the SEI layer on electrodes [23]. Other computational and/or experimental studies regarded the coordination of FTFSI-based ILs with Li ions [24–27], many times in connection with the Raman bands of the aggregates, which were firstly calculated by Giffin et al. for pure ionic liquids [28].

In view of the relatively limited studies of ionic liquids based on the FTFSI anion compared to the FSI and TFSI, we synthesized two new ILs coupling the FTFSI anion with two different quaternary ammonium cations, namely the *N*-trimethyl-*N*-butyl-ammonium, $(N1114)^+$, and the *N*,*N*-diethyl-*N*-methyl-*N*(2-methoxyethyl)-ammonium $(N122(2O1))^+$. The same cations were previously investigated by us in conjunction with the symmetric FSI

and TFSI anions [29–31] and, therefore, a direct comparison of the properties of the derived ionic liquids is feasible. We characterized the new FTFSI ILs concerning their thermal, vibrational and electrochemical stability, liquid range and ionic conductivity.

2. Materials and Methods

The N1114-FTFSI and N122(2O1)-FTFSI ionic liquids were synthesized and purified according to a procedure which uses water as the only processing solvent [32,33]. The precursors *N*-trimethyl-*N*-butyl-ammonium bromide (N1114Br, Solvionic, 99 wt.%) and *N*,*N*-diethyl-*N*-methyl-*N*(2-methoxyethyl)-ammonium bromide (N122(2O1)Br, Solvionic, 99 wt.%) were previously treated trough activated carbon (Sigma-Aldrich, Darco-G60) [33] in deionized water (Millipore ion-exchange resin deionizer). Then, the purified aqueous precursors were reacted with LiFTFSI (Provisco, >98 wt.%) to obtain (anion exchange reaction) the IL materials, which were rinsed with deionized H_2O to remove LiBr, LiFTFSI excess and water-soluble impurities. Finally, the ILs were vacuum dried (oil-free pump) at room temperature for 2 h and, successively, at 80 °C for 48 h. The chemical structure of the $(N1114)^+$ and $N122(2O1)^+$ cations (Figure 1) was validated by ^1H NMR measurements (Figure S1 as Supplementary Data), this confirming the feasibility of the synthesis route. The moisture and bromide content of the ionic liquids, determined by Karl–Fisher titration and X-ray fluorescence according to a route previously reported [33], was found to be lower than 2 and 5 ppm, respectively. The overall purity level of the N1114-FTFSI and N122(2O1)-FTFSI ionic liquids, checked by UV-Vis spectrophotometry measurements as reported in previous work [33], was found to be above 99 wt.%.

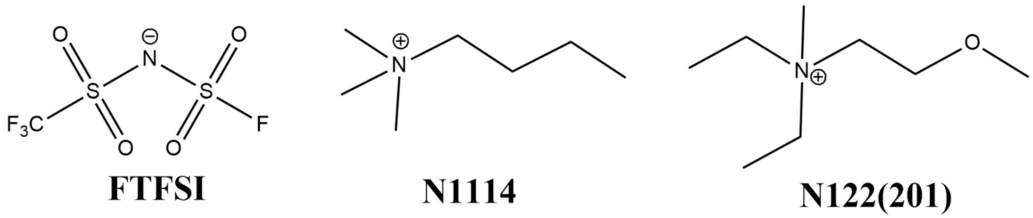

Figure 1. Chemical structure of the $FTFSI^-$ anion, and $N1114^+$ and $N122(2O1)^+$ cations.

The thermal stability of the synthesized ILs was investigated by thermogravimetry. For this purpose, a Setsys Evolution 1200 TGA system by Setaram (KEP Technologies Gropu, Mougins—Sophia Antipolis, France) was used. Measurements were conducted in an argon atmosphere (60 mL/min) with a temperature rate of 10 °C/min and an initial mass of about 25 mg.

The possible presence of low temperature phase transitions was investigated by means of differential scanning calorimetry measurements, using a Mettler Toledo DSC 3 system (Mettler Toledo, Columbus, OH, USA) equipped with a Huber TC100 Cryocooler (Peter Huber Kältemaschinenbau AG, Offenburg, Germany). An argon flux of 50 mL min^{-1} and a temperature rate of 5 °C min^{-1} were applied. The mass of the samples was in the range of about 20 mg.

The ionic conductivity of the ILs and their mixtures with LiTFSI (Solvionic, >99.9 wt.%, battery grade) was investigated as a function of the temperature. The molar fraction of LiTFSI in the LiTFSI-IL mixtures was 0.2, corresponding to a molar concentration around 0.8 M (i.e., close to that of commercial, organic solvent-based LIB electrolytes). The binary LiTFSI-IL electrolytes were prepared in a controlled argon-atmosphere glove-box (Jacomex SAS, Dagneux, France, H_2O and O_2 content < 1 ppm) by dissolving the proper amount of lithium salt in the IL. The electrolytes (handled in the glove-box) were housed in sealed, glass conductivity cells (AMEL 192/K1, Amel Electrochemistry, Milano, Italy) equipped with two porous Pt electrodes (i.e., the cell constant was determined through a 0.1 N KCl aqueous solution). In order to reach a stable low temperature state, the cells were dipped in liquid nitrogen for 30–60 s and then quickly transferred into the climatic chamber (Binder GmbH, Tuttlingen, Germany, MK53, used for the temperature control) at −40 °C [34]. Then,

the cells were kept at −40 °C for at least 18 h prior to starting the conductivity tests, run from −40 to 80 °C at low scan rate (1 °C h^{-1}) for better evidencing the phase transitions [35], through an AMEL 160 conductivity-meter.

The anodic stability of the 0.2LiTFSI-0.8IL electrolytes was investigated using carbon working electrodes (in order to better simulate the situation in battery cells [30]). Electrodes were prepared by blending 70 wt.% Super C45 (IMERYS) and 30 wt.% Na-carboxymethylcellulose (CMC, Dow Wolff Cellulosics, Bomlitz, Germany) in deionized water. The so-obtained slurry was cast onto Al foils (30 µm thick), initially dried in external atmosphere (to massively remove the aqueous solvent). Coin-electrodes (10 mm diameter) were punched and then heated under vacuum at 150 °C overnight (glass oven) prior to being introduced in the glove-box. The electrochemical cells were manufactured (within the glove-box) by housing the carbon electrode, a glass fiber separator (16 mm diameter) and a lithium disk (10 mm diameter) into 2032 MTI containers. The IL electrolyte was initially spread (20 µL) onto the carbon electrode and then dropped (30 µL) onto the separator. Prior to sealing, the cells were subjected to a 30-min vacuum step to allow the full loading of the carbon electrode and separator by the viscous electrolyte. Cyclic voltammetry (CV) tests were carried out on the Li/Carbon cells in the 3.0–5.0 voltage range (1 mV s^{-1}) at 20 °C (Binder climatic chamber).

Infrared spectroscopy measurements were conducted both in the mid- and in the far-infrared range. In the former range, an Agilent 660 spectrometer (Agilent Technologies, Santa Clara, CA, USA) with a DTGS detector and a KBr beamsplitter was used. In the far infrared range, we used the IFS125 spectrometer (Bruker, Billerica, MA, USA) of the AILES beamline of Soleil Synchrotron with a Mylar beamsplitter and a bolometer as detector. For both configurations, the sample was placed in a vacuum tight cell for liquids equipped with diamond optical windows, in order to avoid contaminations from air or moisture. The spectral resolution was fixed to 1 cm^{-1} for both spectrometers. A Specac Variable Temperature Cell (Specac Ltd., Orpington, UK) and a Cryomech cryocooler (Syracuse, NY, USA) allowed us to vary the temperature of the sample in the mid- and in the far-infrared range, respectively.

The infrared spectra of the possible conformers of the FTFSI anion were obtained by means of DFT calculation at the B3LYP level of theory, combined with the 6-31G** basis set. Calculations were performed by means of the Firefly software [36,37]. Starting from the geometry of the three conformers reported by Giffin et al. [28], we re-optimized the structures by means of DFT calculations and the vibration frequencies and the infrared intensity were calculated. To compare the calculated IR spectra with the experimental ones, the former was simulated as the sum of Gaussians curves with maxima at each calculated vibration frequency, a fixed 10 cm^{-1} linewidth and an intensity proportional to the calculated one.

3. Results and Discussion

In the following, the results about the different investigations conducted on the two ionic liquids will be presented and discussed, with the sections divided according to the experimental techniques used for the study.

3.1. Thermal Properties

The thermal stability of the two synthesized samples was investigated by means of thermogravimetric measurements. For comparison, the TGA curves of the ionic liquids containing the same $N1114^+$ cation and the FSI^- or $TFSI^-$ anions or the $N122(2O1)^+$ cation and the TFSI anion are also displayed. The thermal stability of the FTFSI-based ILs (Figure 2) is similar to that of the FSI-based ionic liquid and is much lower than that of the ILs containing the TFSI anion [29]. In fact, one observes a mass reduction of about 2% (1%) around 381 (371) °C in N1114-TFSI, ≈373 (366) °C in N122(2O1)-TFSI, ≈315 (301) °C in N1114-FTFSI, about 304 (288) °C in N1114-FSI and ≈298 (278) °C for N122(2O1)-FTFSI. The lower thermal stability of the FTFSI and FSI ILs is due to the presence in

both anions of at least one SF bond, which is much weaker than the CF_3 bonds present in TFSI. Moreover, both ILs based on the $N122(2O1)^+$ cation have lower decomposition temperatures than those of the materials with the $N1114^+$ cations. The values of the thermal decomposition of the presently investigated ILs based on FTFSI are close to those previously reported for PYR13-FTFSI, PYR14-FTFSI and PYR12O2-FTFSI ranging between 252 and 285 °C for a 1% mass loss [8]. Meister et al. reported that the main decomposition of pure PYR14-FTFSI takes place at 305 °C [9], whereas Al-Masri [38] showed that *N*-isopropyl-*N*-methylpyrrolidinium-FTFSI decomposed above 289 °C. On the other hand, Gao [17] reported a much lower decomposition temperature of ~218 °C for *N*-*N*-diethyl-*N*-methyl-*N*-(2-methoxyethyl)ammonium (fluorosulfonyl)(trifluoromethanesulfonyl)imide. Differently from the other ILs samples, N122(2O1)-FTFSI shows three decomposition steps, likely due to formation of less volatile decomposition products.

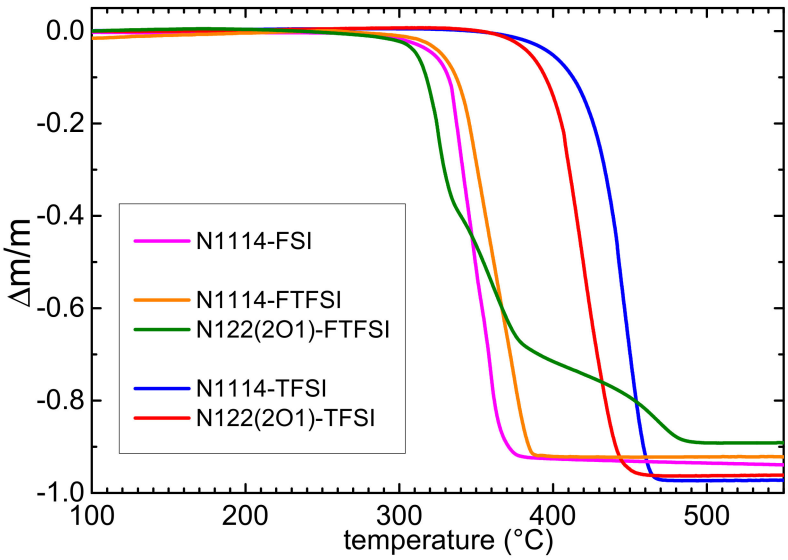

Figure 2. TGA curves of the investigated FTFSI-based ionic liquids in comparison with ILs containing the same cations and the FSI or TFSI anions.

The possible occurrence of low temperature phase transition was studied by means of differential scanning calorimetry. Figure 3 reports the DSC curves measured on heating between −85 and + 50 °C. Neither liquids display marks of melting or glass transition in this temperature range, nor any sign of crystallization on cooling (data not shown). Most likely, this behavior is ascribable to the asymmetric configuration of the $FTFSI^-$ anion [22], which (analogously to that observed in other asymmetric anion ILs [35]) hinders the formation of the IL ion lattice and, consequently, prevents the crystallization process (or lowers the melting temperature). It is plausible that both ILs undergo a glass transition at temperatures lower than the minimum here investigated. This result is in line with the presence of glass transitions in similar ionic liquids based on the FTFSI anion. Indeed, Reiter reported a glass transition temperature between −103 and −107 °C for PYR13-FTFSI, PYR14-FTFSI and PYR12O2-FTFSI [8]; Meister indicated a T_g = −103 °C for PYR14-FTFSI [9], whereas Gao showed that DEME-FTFSI has a glass transition at −107.8 °C [17]. On the other hand, Yunis reported a melting transition (25 °C) and two solid-solid phase transitions in *N*,*N*-Diethylpyrrolidinium(fluorosulfonyl)(trifluoromethanesulfonyl) imide, an IL which possesses a symmetric cation [39]. *N*-isopropyl-*N*-methylpyrrolidinium FTFSI was reported to melt at 25 °C [38]. Al-Masri suggested that a crucial role in the high melting temperature of this IL was played by the branching of the cation alkyl chain [38].

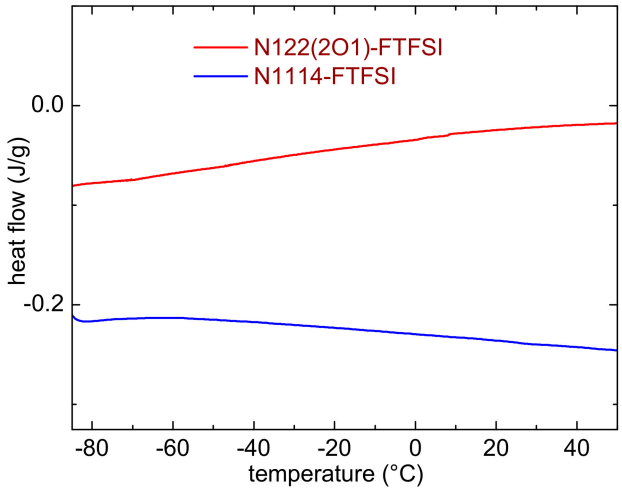

Figure 3. Differential scanning calorimetry curves of the investigated ILs.

3.2. Ionic Conductivity

Figure 4 reports the conductivity vs. temperature dependence (depicted as an Arrhenius plot) of the FTFSI ionic liquids and their mixtures with the LiTFSI salt. No crystalline-liquid phase transition is shown within the whole temperature range investigated, which in agreement with previous DSC measurements. A Vogel−Tammann−Fulcher (VTF) behavior (i.e., absence of a linear dependence) typical of the IL electrolytes [40] is observed even in the presence of the LiTFSI salt, and these results are in good agreement with the DSC data reported in Figure 3. The incorporation of the LiTFSI lithium salt (full data markers in Figure 4) into the pure ILs (open data markers) leads only to a moderate decrease in conductivity. The high charge density on the Li^+ cations (much higher than that of the IL cations) results in the increase of the ion–ion interactions, in turn increasing the viscous drag and, therefore, depleting the ion transport properties [30]. A moderately lower conductivity is shown by the N122(2O1)-FTFSI electrolytes, due to the larger steric hindrance of the $N122(2O1)^+$ cation with respect to $N1114^+$, (leading to higher viscosity). However, interesting conduction values (>10^{-4} S cm^{-1}) are observed already at −10 °C in both FTFSI ionic liquid electrolytes, which approach 10^{-3} S cm^{-1} at 20 °C. This makes the FTFSI-based electrolytes of interest even for low temperature applications.

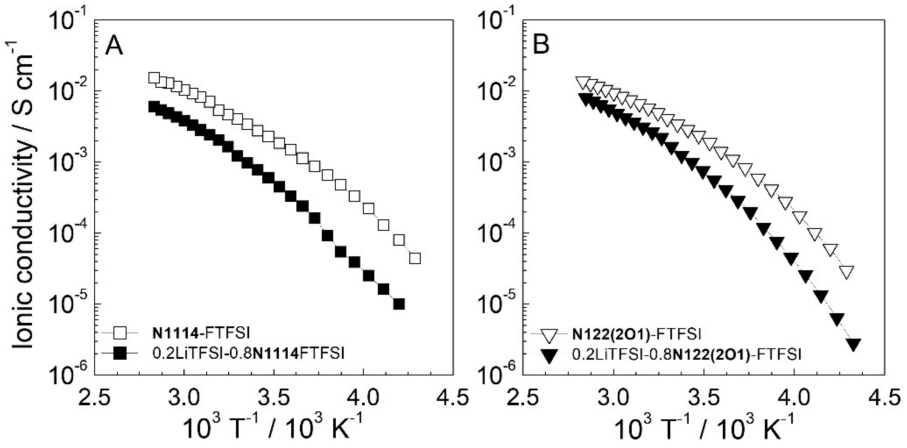

Figure 4. Ionic conductivity vs.temperature dependence, reported as Arrhenius plot, of pure FTFSI ionic liquids and their electrolyte mixtures with the LiTFSI salt (mole fraction equal to 0.2). Panel (**A**): $(N1114)^+$ based electrolytes. Panel (**B**): $(N122(2O1))^+$ based electrolytes. Heating scan rate: 1 C h^{-1}.

3.3. Electrochemical Stability

The anodic stability of the FTFSI ionic liquid electrolytes (IL:LiTFSI mole ratio = 4:1) was investigated through cyclic voltammetries (CVs) carried out using carbon working electrodes. The results, depicted in Figure 5, evidence very low current flows (normalized with respect to the geometrical area of the carbon working electrode) in the first anodic scan. A remarkable reduction inthe current density (<10 μA cm^{-2}) is observed in the following cycles up to the massive degradation (oxidation) of the electrolyte samples occurring around 4.8 V vs. the $Li^+/Li°$ redox couple), and no other feature is observed. This indicates an excellent anodic stability up to 4.8 V and suggests that the irreversible oxidation processes taking place during the first anodic scan are likely associated to impurities, even if in very low content, rather than to the ionic liquids and/or the LiTFSI salt [30]. The drastic decay of the current flow through the cell after the first anodic sweep also supports a high purity content of the investigated samples. Overall, the FTFSI electrolytes show electrochemical robustness against oxidation up to 4.8 V, this making them appealing for high operative voltage lithium battery systems.

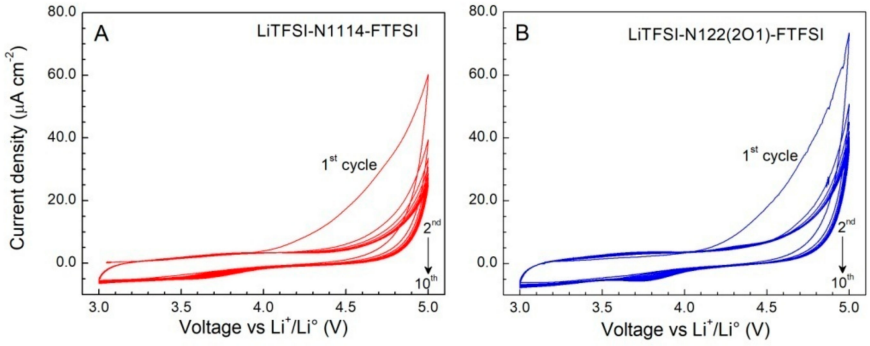

Figure 5. Anodic cyclic voltammetries of the 0.2LiTFSI-0.8N1114-FTFSI (panel (**A**)) and 0.2LiTFSI-0.8N122(2O1)-FTFSI (panel (**B**)) ionic liquid electrolytes. Carbon and lithium metal are used as the working electrode and the counter electrode, respectively. Scan rate: 1 mV s^{-1}. Temperature: 20 °C. The current density value was obtained by normalizing the current flow with respect to the geometrical surface area of the working electrode.

3.4. Vibrational Properties

The three possible structures of conformers identified by Giffin [28] were re-optimized by means of DFT calculations at the B3LYP/6-31G** level. The relative energies of the three conformers, the vibrational frequencies and infrared intensities are reported in Tables S1 and S2 of the Supplementary Materials. The difference between the conformers comes from the different FSSC dihedral angle, which is equal to 153.2 (anti configuration), −40.6 (gauche) and 6.1 (syn)° for Conf_A, Conf_B and Conf_C, which have relative energies of 0.0, +1.1 and +2.9 kJ/mol (see Table S1 of the Supplementary Materials). These values are in line with those reported in the only study about conformers of FTFSI, which is available in the literature [28].

The temperature dependence of the mid-infrared spectra of the two ILs are reported in Figure 6, together with the calculated absorbance of the three conformers of FTFSI. The far-infrared spectrum could be measured only for N1114-FTFSI and is reported in Figure 7, in comparison with the computational results. Figures 6 and 7 display a good correspondence between the expected vibrational lines of the FTFSI conformers and the measured absorbance lines in the whole energy range, provided that the frequencies of the calculated absorptions are scaled by a factor of 1.04 for the mid-infrared or 1.065 for the far-infrared. This procedure is usually performed for comparing calculated and experimentally measured spectra.

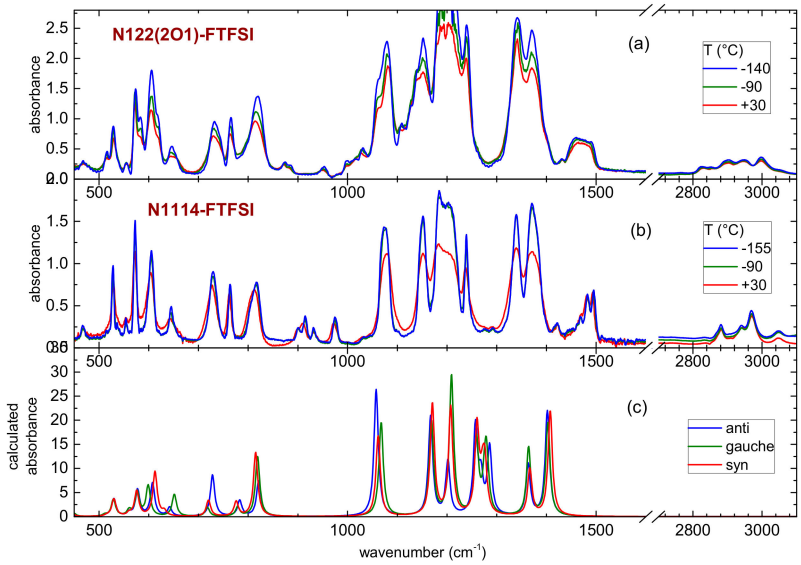

Figure 6. Temperature dependence of the mid-infrared spectrum of N122(2O1)-FTFSI (panel (**a**)) and N1114-FTFSI (panel (**b**)) and comparison with the calculated absorbance of the three conformers of the FTFSI anion (panel (**c**)); a scaling factor of 1.04 was used for the calculated frequencies.

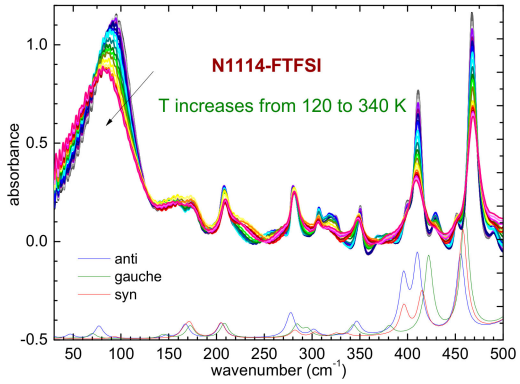

Figure 7. Temperature dependence of the far-infrared spectrum of N1114-FTFSI (upper part) and comparison with the calculated absorbance of the three conformers of the FTFSI anion (lower part); a scaling factor of 1.065 was used for the calculated frequencies.

Analogously to the case of many ionic liquids containing other fluorinated anions, like TFSI or FSI, the infrared spectrum is dominated by the absorption lines of the anion, except above 1400 cm^{-1}, where one can find NH, CH or OH bending and stretching bands, usually coming from the cations. Moreover, a limited spectral region between 800 and 1050 cm^{-1} is usually free from the vibrations of the anions, thus containing vibrations only belonging to the cations. Indeed, these spectral regions are those presenting different absorption bands, due to the occurrence of different cations in the two ILs.

Figures 6 and 7 show that despite there is a clear narrowing of all absorption lines at low temperatures, there are no disappearing bands or abrupt changes inthe spectra. This fact further suggests that no crystallization of the ILs occurs even at the lowest temperatures investigated here, which is in agreement with the previously reported DSC results and further extending the investigated temperature range. Moreover, the vibrational bands of the three conformers of FTFSI are very close to each other, and it is not possible to identify clear spectral marks of any of the conformers of FTFSI. This is different from the TFSI anion, for which clear marks of the two cis and trans conformers are visible in the infrared spectra [41]. Instead, for FSI, the infrared spectra of its two conformers are rather superimposed, and the lines found in the experimental spectra come from the superposition

of the contribution from the two rotamers [42]. The infrared spectrum of FTFSI-based ionic liquids, to the best of our knowledge, has never been reported before. However, some vibrational properties obtained by means of Raman spectroscopy were reported by Giffin et al. [28]. Moreover, these authors concluded that the vibrations of the three conformers of FTFSI are highly superimposed and, possibly, a Raman line centered around 740 cm^{-1} could be composed of the contributions from two conformers [28].

A last remark concerns the temperature evolution of the far-infrared spectrum below 200 cm^{-1}, as reported in Figure 7. In this region of the spectrum, one usually observes a broad peak centered around 90 cm^{-1}, which was attributed to the dispersion forces acting in the ILs [31,41,42]. In the case of hydrogen bonding occurring in the ionic liquids, two side bands centered around 50 and 120 cm^{-1} can also be present [31,41,42]. In N1114-FTFSI, these side bands seem to not be present and the temperature evolution is similar to that reported for N122(2O1)-TFSI, where the peak centered around 80 cm^{-1} does not split at low temperatures but shifts towards higher frequencies as the temperature is reduced [31]. This fact was interpreted as an evidence that hydrogen bonding is not energetically favored in N122(2O1)-TFSI [31]. In view of the previous findings, we can suggest that in the presently investigated N1114-FTFSI hydrogen bonding also does not play a central role among the inter- and intra- molecular interactions.

4. Conclusions

Two novel ionic liquids, N1114-FTFSI and N122(2O1)-FTFSI, were synthesized by an anion exchange reaction in water. The purity of the liquids was higher than 99 wt.% and the water content lower than 5 ppm. The mass loss measured on heating did not exceed 2% below ~300 °C. Both ILs did not crystallize on cooling down to −90 °C, as witnessed by DSC measurements. Infrared spectra as a function of temperature suggests that crystallization does not occur even down to −140 °C. For both ILs, the ionic conductivity was higher than 10^{-4} S cm^{-1} already at −10 °C, suggesting the possible application as a low temperature electrolyte. Moreover, a high anodic stability, up to about 4.8 V vs. Li, of the mixtures with the LiTFSI salt was obtained. This fact confirms that ILs based on the FTFSI anion are appealing for realizing safer and highly reliable lithium battery systems operating at high voltages.

Supplementary Materials: The following supporting information can be downloaded at: https://www.mdpi.com/article/10.3390/app12094524/s1, Figure S1. NMR spectra of N1114Br (panel a) and N122(2O1)-TFSI (panel b). Both spectra comply with the molecular structures and no impurity is detected. Table S1: Relative energy of the conformers of FTFSI calculated by DFT calculations in vacuum at the B3LYP/6-31G** level and the corresponding FSSC dihedral angle; Table S2: Frequencies and infrared intensities of the three conformers of FTFSI, calculated by DFT calculations at the B3LYP/6-31G** level in vacuum.

Author Contributions: Conceptualization, G.B.A. and A.P.; methodology, G.B.A., O.P. and A.P.; validation, all authors; formal analysis, G.B.A., G.M. and A.P.; investigation, all authors; resources, D.B., F.L., A.F., R.L. and S.F.; data curation, G.B.A., G.M. and A.P.; writing—original draft preparation, G.B.A., O.P. and A.P.; visualization, G.B.A. and A.P.; funding acquisition, G.B.A. and A.P. All authors have read and agreed to the published version of the manuscript.

Funding: The authors would like to acknowledge the financial support from the European Union Horizon 2020 research and innovation program within the Si-DRIVE project, grant agreement No 814464, and the CALIPSOplus project, grant agreement No. 730872, for the beamtime 20210260 and 20200422 at SOLEIL Synchrotron.

Institutional Review Board Statement: Not applicable.

Informed Consent Statement: Not applicable.

Data Availability Statement: Data is contained within the article or Supplementary Materials.

Conflicts of Interest: The authors declare no conflict of interest.

References

1. Welton, T. Ionic liquids: A brief history. *Biophys. Rev.* **2018**, *10*, 691–706. [CrossRef] [PubMed]
2. Pešić, J.; Watson, M.; Papović, S.; Vraneš, M. Ionic Liquids: Review of their Current and Future Industrial Applications and their Potential Environmental Impact. *Recent Pat. Nanotechnol.* **2021**, *15*, 225–244. [CrossRef] [PubMed]
3. Singh, S.K.; Savoy, A.W. Ionic liquids synthesis and applications: An overview. *J. Mol. Liq.* **2020**, *297*, 112038. [CrossRef]
4. Fabre, E.; Sohel Murshed, S.M. A review of the thermophysical properties and potential of ionic liquids for thermal applications. *J. Mater. Chem. A* **2021**, *9*, 15861–15879. [CrossRef]
5. Tiago, G.A.O.; Matias, I.A.S.; Ribeiro, A.P.C.; Martins, L.M.D.R.S. Application of Ionic Liquids in Electrochemistry—Recent Advances. *Molecules* **2020**, *25*, 5812. [CrossRef]
6. Armand, M.; Endres, F.; MacFarlane, D.R.; Ohno, H.; Scrosati, B. Ionic-liquid materials for the electrochemical challenges of the future. *Nat. Mater.* **2009**, *8*, 621–629. [CrossRef]
7. Jeremias, S.; Carewska, M.; Conte, L.; Passerini, S.; Appetecchi, G.B. Asymmetry effect of novel per(fluoroalkylsulfonyl)imide anions in pyrrolidinium ionic liquids. *RSC Adv.* **2013**, *3*, 17755–17761. [CrossRef]
8. Reiter, J.; Jeremias, S.; Paillard, E.; Winter, M.; Passerini, S. Fluorosulfonyl-(trifluoromethanesuldonyl)imide ionic liquids with enhanced asymmetry. *Phys. Chem. Chem. Phys.* **2013**, *15*, 2565–2571. [CrossRef]
9. Meister, P.; Siozios, V.; Reiter, J.; Klamor, S.; Rothermel, S.; Fromm, O.; Meyer, H.-W.; Winter, M.; Placke, T. Dual-Ion Cells based on the Electrochemical Intercalation of Asymmetric Fluorosulfonyl-(trifluoromethanesulfonyl) imide Anions into Graphite. *Electrochim. Acta* **2014**, *130*, 625–633. [CrossRef]
10. Meister, P.; Schmuelling, G.; Winter, M.; Placke, T. New insights into the uptake/release of FTFSI−anions into graphite by means of in situ powder X-ray diffraction. *Electrochem. Commun.* **2016**, *71*, 52–55. [CrossRef]
11. Kühnel, R.S.; Reiter, J.; Jeong, S.; Passerini, S.; Balducci, A. Anodic stability of aluminum current collectors in an ionic liquid based on the (fluorosulfonyl)(trifluoromethanesulfonyl)imide anion and its implication on high voltage supercapacitors. *Electrochem. Commun.* **2014**, *38*, 117–119. [CrossRef]
12. Eshetu, G.; Grugeon, S.; Kim, H.; Jeong, S.; Wu, L.; Gachot, G.; Laruelle, S.; Armand, M.; Passerini, S. Comprehensive Insights into the Reactivity of Electrolytes Based on Sodium Ions. *ChemSusChem* **2016**, *9*, 462–471. [CrossRef]
13. Meister, P.; Qi, X.; Kloepsch, R.; Krmer, E.; Streipert, B.; Winter, M.; Placke, T. Anodic Behavior of the Aluminum Current Collector in Imide-Based Electrolytes: Influence of Solvent, Operating Temperature, and Native Oxide-Layer Thickness. *ChemSusChem* **2017**, *10*, 804–814. [CrossRef]
14. Di Lecce, D.; Sharova, V.; Jeong, S.; Moretti, A.; Passerini, S. A multiple electrolyte concept for lithium-metal batteries. *Solid State Ion.* **2018**, *316*, 66–74. [CrossRef]
15. Eshetu, G.G.; Judez, X.; Li, C.; Martinez-Ibañez, M.; Gracia, I.; Bondarchuk, O.; Carrasco, J.; Rodriguez-Martinez, L.M.; Zhang, H.; Armand, M. Ultrahigh Performance All Solid-State Lithium Sulfur Batteries: Salt Anion's Chemistry-Induced Anomalous Synergistic Effect. *J. Am. Chem. Soc.* **2018**, *140*, 9921–9933. [CrossRef]
16. Ma, Q.; Fang, Z.; Liu, P.; Ma, J.; Qi, X.; Feng, F.; Nie, J.; Hu, J.-S.; Li, H.; Huang, X.; et al. Improved Cycling Stability of Lithium-Metal Anode with Concentrated Electrolytes Based on Lithium(Fluorosulfonyl)(trifluoromethanesulfonyl)imide. *ChemElectroChem* **2016**, *3*, 531–536. [CrossRef]
17. Gao, X.; Wu, F.; Mariani, A.; Passerini, S. Concentrated Ionic-Liquid-Based Electrolytes for High-Voltage Lithium Batteries with Improved Performance atRoom Temperature. *ChemSusChem* **2019**, *12*, 4185–4193. [CrossRef]
18. Chidiac, J.; Timperman, L.; Anouti, M. Small dissymmetry, yet large effects on the transport properties of electrolytes based on imide salts: Consequences on performance in Li-ion batteries. *J. Energy Chem.* **2022**, *65*, 352–366. [CrossRef]
19. Chidiac, J.; Timperman, L.; Anouti, M. Physical properties and compatibility with graphite and lithium metal anodes of non-flammable deep eutectic solvent as a safe electrolyte for high temperature Li-ion batteries. *Electrochim. Acta* **2022**, *408*, 139944. [CrossRef]
20. Forsyth, M.; Hilder, M.; Zhang, Y.; Chen, F.; Carre, L.; Rakov, D.A.; Armand, M.; Macfarlane, D.R.; Pozo-Gonzalo, C.; Howlett, P.C. Tuning Sodium Interfacial Chemistry with Mixed-Anion Ionic Liquid Electrolytes. *ACS Appl. Mater. Interfaces* **2019**, *11*, 43093–43106. [CrossRef]
21. Umesh, B.; Chandra Rath, P.; Patra, J.; Hernandha, R.F.H.; Majumder, S.B.; Gao, X.; Bresser, D.; Passerini, S.; Lai, H.Z.; Chang, T.-L.; et al. High-Li+-fraction ether-side-chain pyrrolidinium–asymmetric imide ionic liquid electrolyte for high-energy-density Si//Ni-rich layered oxide Li-ion batteries. *Chem. Eng. J.* **2022**, *430*, 132693. [CrossRef]
22. Jeong, S.-S.; Li, S.; Appetecchi, G.B.; Passerini, S. Asymmetric, quaternary, ammonium-based ionic liquids as electrolyte components for safer, high-energy lithium batteries. *Energy Storage Mater.* **2019**, *18*, 1–9. [CrossRef]
23. Rigoni, A.S.; Breedon, M.; Collis, G.E.; Spencer, M.J.S. The interaction of several fluorinated ionic liquids on the LiF(001) surface. *Surf. Interfaces* **2021**, *22*, 100836. [CrossRef]
24. Giffin, G.A.; Moretti, A.; Jeong, S.; Pilar, K.; Brinkkötter, M.; Greenbaum, S.G.; Schönhoff, M.; Passerini, S. Connection between Lithium Coordination and Lithium Diffusion in [Pyr12O1][FTFSI] Ionic Liquid Electrolytes. *ChemSusChem* **2018**, *11*, 1981–1989. [CrossRef] [PubMed]
25. Penley, D.; Vicchio, S.P.; Getman, R.B.; Gurkan, B. Energetics of Li + Coordination with Asymmetric Anions in Ionic Liquids by Density Functional Theory. *Front. Energy Res.* **2021**, *9*, 725010. [CrossRef]

26. Reber, D.; Takenaka, N.; Kühnel, R.S.; Yamada, A.; Battaglia, C. Impact of Anion Asymmetry on Local Structure and Supercooling Behavior of Water-in-Salt Electrolytes. *J. Phys. Chem. Lett.* **2020**, *11*, 4720–4725. [CrossRef] [PubMed]
27. Brinkkötter, M.; Giffin, G.A.; Moretti, A.; Jeong, S.; Passerini, S.; Schönhoff, M. Relevance of ion clusters for Li transport atelevated salt concentrations in [Pyr12O1][FTFSI]ionic liquid-based electrolytes. *Chem. Commun.* **2018**, *54*, 4278–4281. [CrossRef]
28. Giffin, G.A.; Laszczynski, N.; Jeong, S.; Jeremias, S.; Passerini, S. Conformations and Vibrational Assignments of the (Fluorosulfonyl)(trifluoromethanesulfonyl)imide Anion in Ionic. Liquids. *J. Phys. Chem. C* **2013**, *117*, 24206–24212. [CrossRef]
29. Cimini, A.; Palumbo, O.; Simonetti, E.; De Francesco, M.; Appetecchi, G.B.; Fantini, S.; Lin, R.; Falgayrat, A.; Paolone, A. Decomposition temperatures and vapour pressures of selected ionic liquids for electrochemical applications. *J. Therm. Anal. Calorim.* **2020**, *142*, 1791–1797. [CrossRef]
30. Brutti, S.; Simonetti, E.; De Francesco, M.; Sarra, A.; Paolone, A.; Palumbo, O.; Fantini, S.; Lin, R.; Falgayrat, A.; Choi, H.; et al. Ionicliquidelectrolytes for high-voltage, lithium-ionbatteries. *J. Power Sources* **2020**, *479*, 228791. [CrossRef]
31. Palumbo, O.; Sarra, A.; Brubach, J.B.; Trequattrini, F.; Cimini, A.; Brutti, S.; Appetecchi, G.B.; Simonetti, E.; Maresca, G.; Fantini, S.; et al. So similar, yet so different: The case of the ionic liquids *N*-trimethyl-N(2-methoxyethyl) ammonium bis(trifluoromethanesulfonyl)imide and *N*,*N*-diethyl-*N*-methyl-*N*(2-methoxyethyl) ammonium bis(trifluoromethanesulfonyl)imide. *Front. Phys.* **2022**, *10*, 851279. [CrossRef]
32. Montanino, M.; Alessandrini, F.; Passerini, S.; Appetecchi, G.B. Water-based synthesis of hydrophobic ionic liquids for high-energy electrochemical devices. *Electrochim. Acta* **2013**, *96*, 124–133. [CrossRef]
33. De Francesco, M.; Simonetti, E.; Giorgi, G.; Appetecchi, G.B. About purification route of hydrophobic ionic liquids. *Challenges* **2017**, *8*, 11. [CrossRef]
34. Henderson, W.A.; Passerini, S. Phase behavior of ionic liquid−LiX mixtures: Pyrrolidinium cations and TFSI-anions. *Chem. Mater.* **2004**, *16*, 2881–2885. [CrossRef]
35. Appetecchi, G.B.; Montanino, M.; Zane, D.; Carewska, M.; Alessandrini, F.; Passerini, S. Effect of the alkyl group on the synthesis and the electrochemical properties of *N*-alkyl-*N*-methyl-pyrrolidinium bis(trifluromethansulfonyl)imide ionic liquids. *Electrochim. Acta* **2009**, *54*, 1325–1332. [CrossRef]
36. Granovsky, A.A. Firefly Version 8.0. Available online: http://classic.chem.msu.su/gran/firefly/index.html (accessed on 7 March 2022).
37. Schmidt, M.W.; Baldridge, K.K.; Boatz, J.A.; Elbert, S.T.; Gordon, M.S.; Jensen, J.H.; Koseki, S.; Matsunaga, N.; Nguyen, K.A.; Su, S.; et al. General Atomic and Molecular Electronic Structure System. *Comput. Chem.* **1993**, *14*, 1347–1363. [CrossRef]
38. Al-Masri, D.; Yunis, R.; Hollenkamp, A.F.; Doherty, C.M.; Pringle, J.M. The influence of alkyl chain branching on the properties of pyrrolidinium-based ionic electrolytes. *Phys. Chem. Chem. Phys.* **2020**, *22*, 18102–18113. [CrossRef]
39. Yunis, R.; Newbegin, T.W.; Hollenkamp, A.F.; Pringle, J.M. Ionic liquids and plastic crystals with a symmetrical pyrrolidinium cation. *Mater. Chem. Front.* **2018**, *2*, 1207–1214. [CrossRef]
40. Appetecchi, G.B.; Montanino, M.; Passerini, S. Ionic Liquid-based Electrolytes for High-Energy Lithium Batteries. In *Ionic Liquids Science and Applications*; ACS Symposium Series 1117; Visser, A.E., Bridges, N.J., Rogers, R.D., Eds.; Oxford University Press Inc.: Oxford, UK; American Chemical Society: Washington, DC, USA, 2013.
41. Palumbo, O.; Cimini, A.; Trequattrini, F.; Brubach, J.-B.; Roy, P.; Paolone, A. Evidence of the CH···O Hydrogen Bonding in Imidazolium-Based Ionic Liquids from Far-Infrared Spectroscopy Measurements and DFT Calculations. *Int. J. Mol. Sci.* **2021**, *22*, 6155. [CrossRef]
42. Palumbo, O.; Trequattrini, F.; Cimini, A.; Tsurumaki, A.; Navarra, A.; Paolone, A. Inter- and Intramolecular Interactions in Ether-Functionalized Ionic Liquids. *J. Phys. Chem. B* **2021**, *125*, 2380–2388. [CrossRef]